6
Results

The expected damage on a critical point of the drilling tower shown on Fig. 4.2 will be calculated. The working life of the equipment is 20 years. The main parameters of the platform and of the tower are shown on Tab. 6.1.

Table 6.1: Main parameters of the equipment

Diameter of the legs of the platform	D_c	27 m
Distance between the legs X dir.	L	70 m
Distance between the legs Y dir.	L	50 m
Draft of the platform	DR	15 m
Mass of the platform	M_P	15.000 t
Height of the tower	H	60 m
Height of the cross section	h	8 m
Width of the cross section	$b(x)$	7 m to 6 m
Thickness of the plates of the tower	t	24 mm to 15 mm
Mass of the drilling tower	M_t	266 t
Hydrodynamic mass coefficient	a	760 t
Hydrodynamic damping coefficient	b	68 t/s
Weibull parameter for H_s	γ	0.84
Weibull parameter for H_s	m	1.6
Weibull parameter for H_s	β	1.6
S-N curve parameter	m_{f1}	3
S-N curve parameter	C_{f1}	$10^{12.592}$
S-N curve parameter	m_{f2}	5
S-N curve parameter	C_{f2}	$10^{16.320}$
Stress concentration factor	SCF	1

The Pierson-Moskowitz spectrum has been used to identify the frequency composition of the sea surface wave elevation. The spectrum is shown on Fig. 6.1.

Using this spectrum, the sea surface elevation in an area of 100 by 100m was calculated. On Fig. 6.2 a snapshot of the sea surface elevation in this area is shown.

After the calculation of the sea surface elevation, a KL decomposition of the sea surface elevation was accomplished. The results have been approximated using only 6 modes. The construction of KL basis took 5% of the neces-

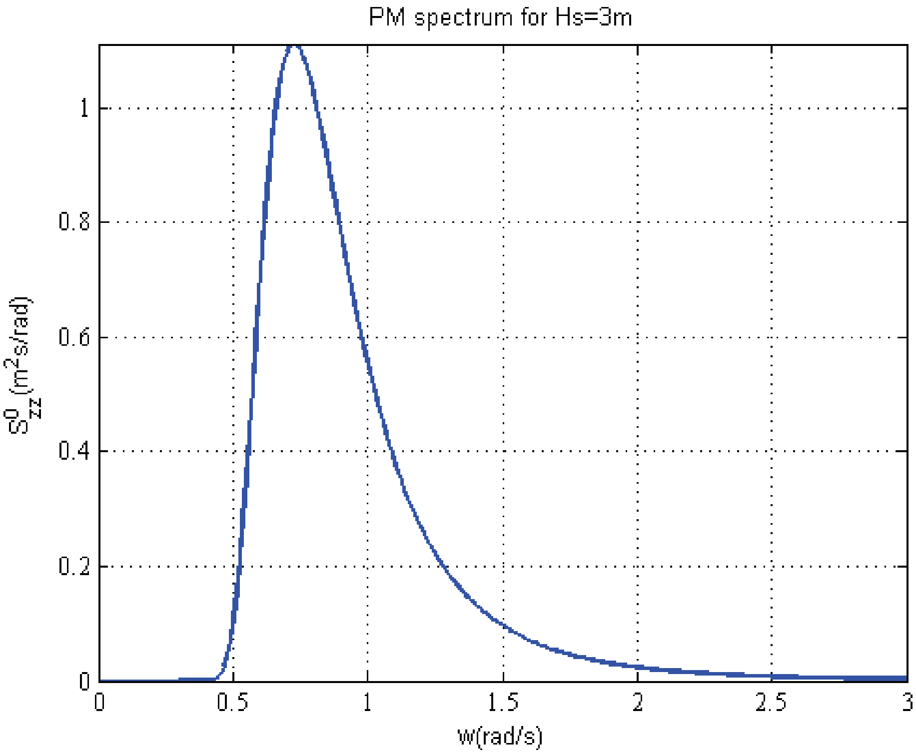

Figure 6.1: PM spectrum

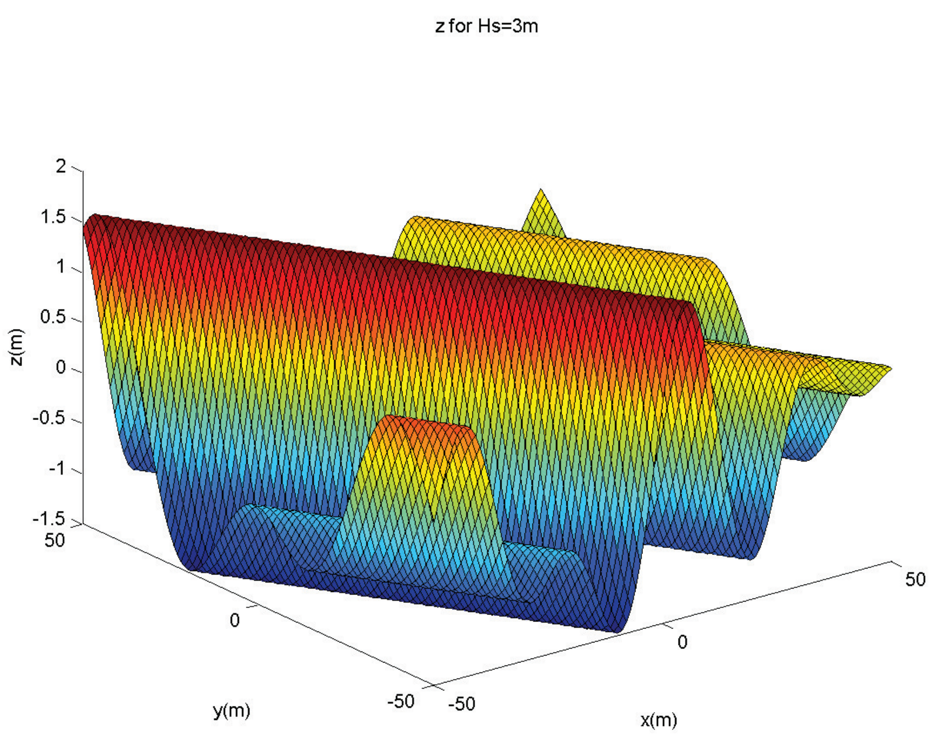

Figure 6.2: Sea surface elevation

sary time to calculate the original elevation. On Fig. 6.3 one can see a comparison between the original elevation and the result obtained from reduced-order model. The results are compared at a grid of 10 by 10 points equally spaced, therefore a total of 100 points have been compared. A good agreement between both results can be noted.

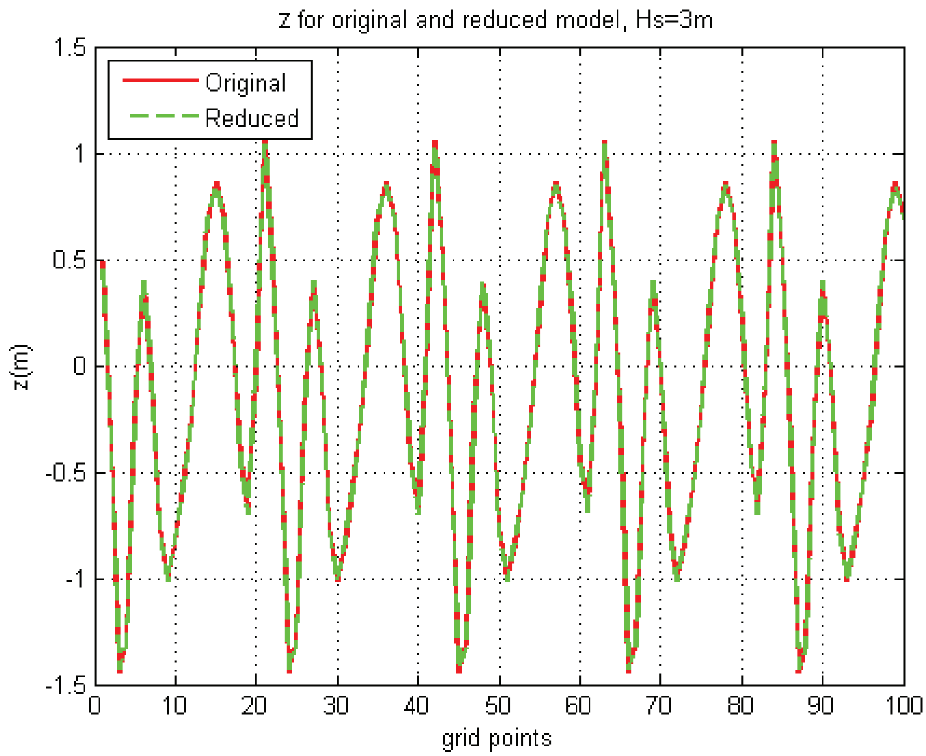

Figure 6.3: Original x reduced-order model

The Weibull parameters for the distribution of the significant wave heights at the area where the structure will be installed are given on Tab. 6.1. The expected working years per each significant wave height are shown on Tab. 6.2.

Table 6.2: Significant wave height probability

$H_S(m)$	Prob.	Working years	$H_S(m)$	Prob.	Working years
1	0.0248	$t_1 = 0.496$	5	0.0413	$t_5 = 0.827$
2	0.4252	$t_2 = 8.503$	6	0.0084	$t_6 = 0.169$
3	0.3514	$t_3 = 7.028$	7	0.0013	$t_7 = 0.026$
4	0.1474	$t_4 = 2.948$	8	0.0002	$t_8 = 0.003$

It was considered that there is no prevailing direction for the waves. This choice applies for moored platforms on locations where there are no prevailing wind directions. Therefore, within the period that each significant wave height takes place, the probability of occurrence of the direction of the waves was considered to be equally distributed. Due to the symmetry of the model, only the directions of waves ranging for 0 to 90 degrees have been considered, and in order to simplify the calculations it was considered that the directions of 0, 22.5, 45, 67.5 and 90 degrees take place for 20% of the expected period for each significant wave height. A realization of the sea surface elevation at two of the cylinders of the platform is shown on Fig. 6.4.

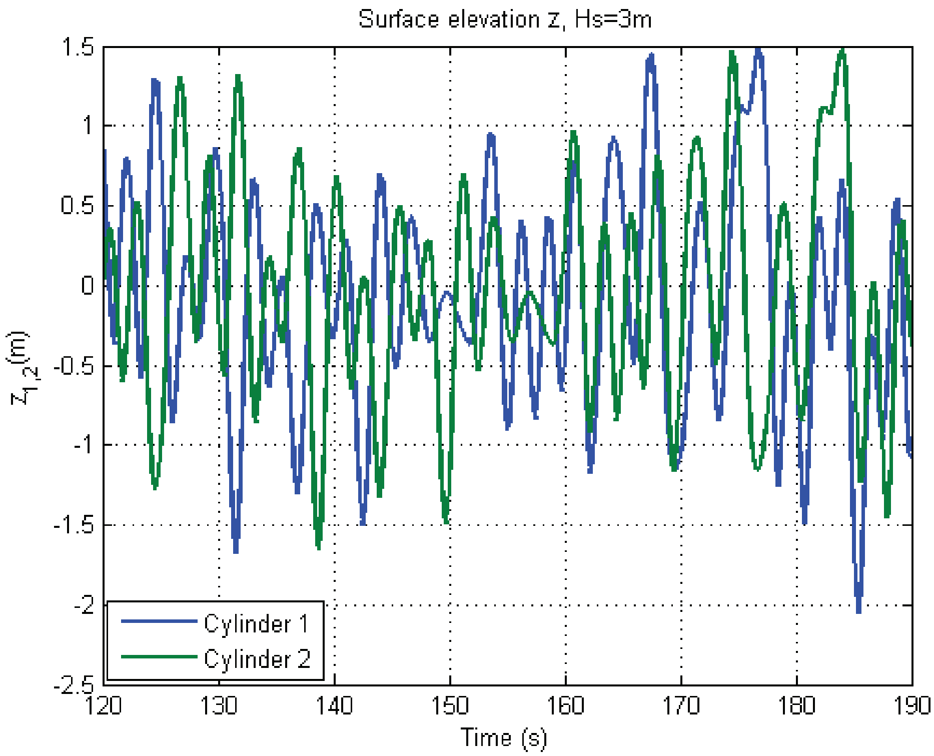

Figure 6.4: Sea surface elevation at cylinders

The Froude-Krilov forces on the bottom of the cylinders and the two additional components, one proportional to the effective vertical acceleration and one proportional to the effective vertical velocity of the cylinders, are the only external forces acting on the platform. A realization of the total wave loads over the cylinders is shown on Fig. 6.5. Due to the two additional components other than the Froude-Krilov forces, the frequencies of the total wave loads are lower than the frequencies of the sea surface elevation.

The dynamics of the platform is given by Eq. (6.1). The restitution coefficient is given by Eq. (3.35). The remaining parameters are given on Tab. 6.1.

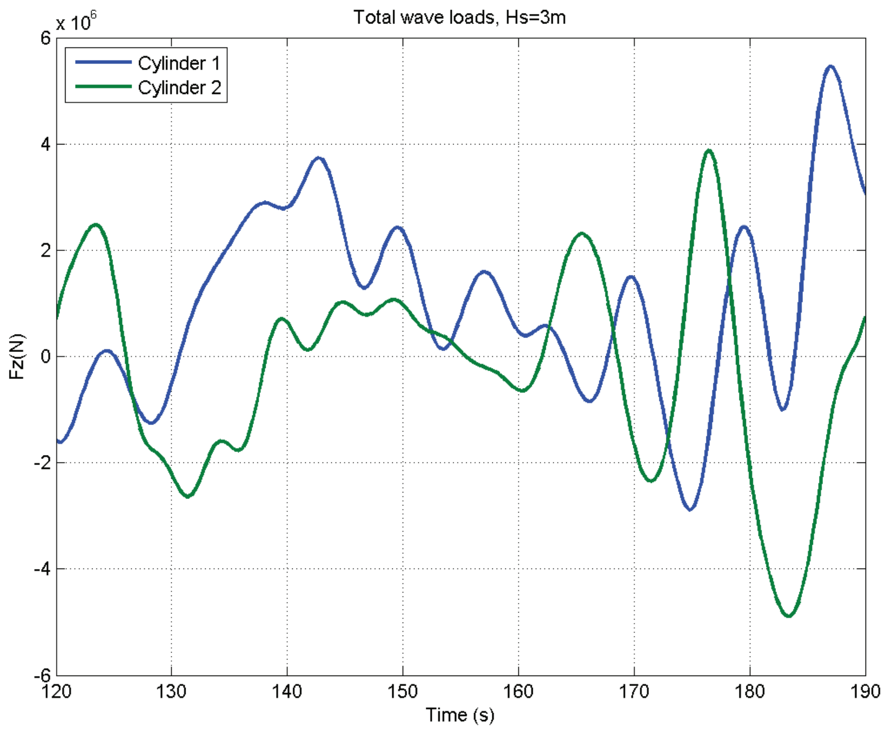

Figure 6.5: Total wave loads

$$\begin{bmatrix} M_P + 4a & 0 & 0 \\ 0 & I_{xx} + 2aL_y^2 & -I_{xy} \\ 0 & -I_{xy} & I_{xx} + 2aL_x^2 \end{bmatrix} \begin{Bmatrix} \ddot{z} \\ \ddot{\phi} \\ \ddot{\theta} \end{Bmatrix} + \begin{bmatrix} 4b & 0 & 0 \\ 0 & 2bL_y^2 & 0 \\ 0 & 0 & 2cL_x^2 \end{bmatrix} \begin{Bmatrix} \dot{z} \\ \dot{\phi} \\ \dot{\theta} \end{Bmatrix} + \begin{bmatrix} 4c & 0 & 0 \\ 0 & 2cL_y^2 & 0 \\ 0 & 0 & 2cL_x^2 \end{bmatrix} \begin{Bmatrix} z \\ \phi \\ \theta \end{Bmatrix} = \begin{Bmatrix} (F_1 + F_2 + F_3 + F_4) \\ (-F_1 - F_2 + F_3 + F_4)\, L_y \\ (-F_1 + F_2 - F_3 + F_4)\, L_x \end{Bmatrix} \tag{6.1}$$

The steady-state part of one realization of the platform displacement is shown on Fig. 6.6, and the steady-state part of one realization of the platform rotation is shown on Fig. 6.7. The platform displacement depends on the summation of the total wave loads over the cylinders, and the platform rotation depends on the differences between the total wave loads over the cylinders.

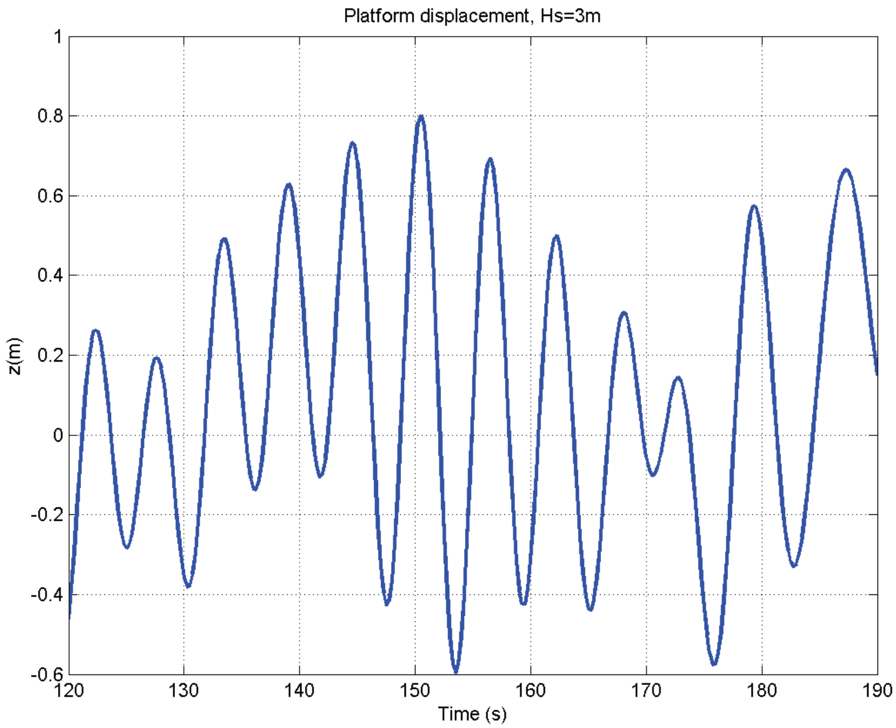

Figure 6.6: Platform displacement

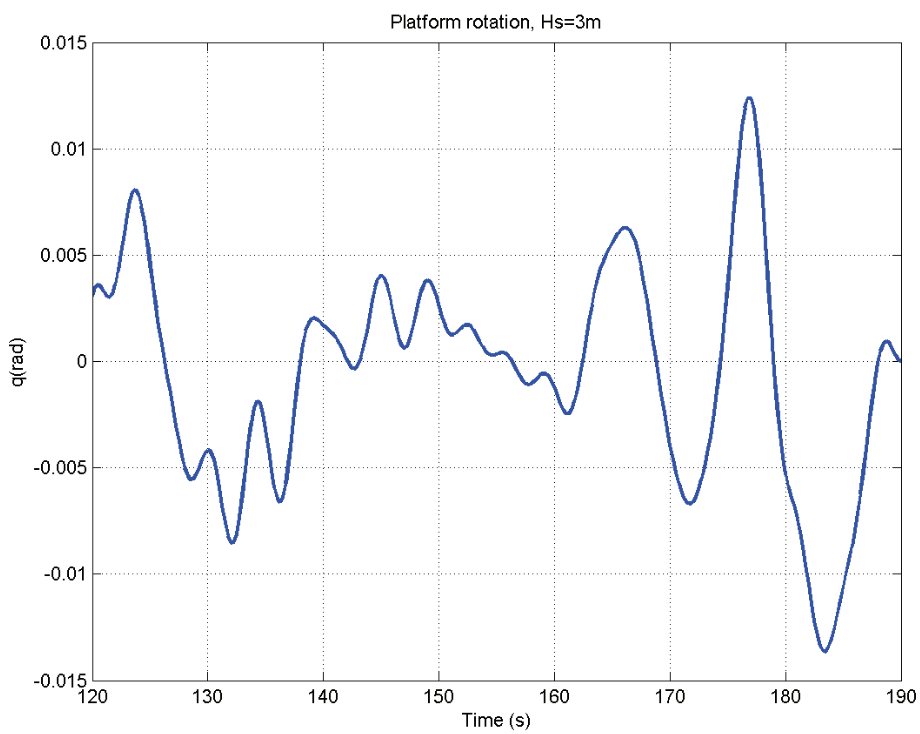

Figure 6.7: Platform rotation

The lifting load will be considered a concentrated mass at the free end of the beam/drilling tower. As the equipment is not always lifting the maximum load and there are limitations for the maximum load depending on the sea condition, it is necessary to estimate during design phase of the equipment the rate of use of the equipment for each expected sea condition. The maximum lifting load of the equipment is 800ton and this is the maximum value of the concentrated mass, M_c. The rates of utilization of the equipment under each sea condition are given on Tab. 6.3.

Table 6.3: Rates of utilization of the equipment

Condition	-	1	2	3	4	5	6	7	8	9	10
h_S	m	1	1	1	1	1	2	2	2	2	2
Time	years	$\frac{t_1}{5}$	$\frac{t_1}{5}$	$\frac{t_1}{5}$	$\frac{t_1}{5}$	$\frac{t_1}{5}$	$\frac{t_2}{5}$	$\frac{t_2}{5}$	$\frac{t_2}{5}$	$\frac{t_2}{5}$	$\frac{t_2}{5}$
Conc. mass	ton	0	$\frac{M_c}{4}$	$\frac{M_c}{2}$	$\frac{3M_c}{4}$	M_c	0	$\frac{M_c}{4}$	$\frac{M_c}{2}$	$\frac{3M_c}{4}$	M_c
Condition	-	11	12	13	14	15	16	17	18	19	20
h_S	m	3	3	3	3	3	4	4	4	4	4
Time	years	$\frac{t_3}{5}$	$\frac{t_3}{5}$	$\frac{t_3}{5}$	$\frac{t_3}{5}$	$\frac{t_3}{5}$	$\frac{t_4}{5}$	$\frac{t_4}{5}$	$\frac{t_4}{5}$	$\frac{t_4}{5}$	$\frac{t_4}{5}$
Conc. mass	ton	0	$\frac{M_c}{4}$	$\frac{M_c}{2}$	$\frac{3M_c}{4}$	M_c	0	$\frac{M_c}{4}$	$\frac{M_c}{2}$	$\frac{3M_c}{4}$	M_c
Condition	-	21	22	23	24	25	26	27	28		
h_S	m	5	5	5	6	6	6	7	8		
Time	years	$\frac{t_5}{3}$	$\frac{t_5}{3}$	$\frac{t_5}{3}$	$\frac{t_6}{3}$	$\frac{t_6}{3}$	$\frac{t_6}{3}$	t_7	t_8		
Conc. mass	ton	0	$\frac{M_c}{4}$	$\frac{M_c}{2}$	0	$\frac{M_c}{4}$	$\frac{M_c}{2}$	0	0		

After the definition of the expected working conditions, the dynamic simulations using a reduced order model for the finite element model was accomplished. A realization of the time history of the stress cycles at the critical point is shown on Fig. 6.8.

The steady-state part of the response is a stationary and ergodic process, therefore only one realization is needed, since a convergence check is accomplished. An histogram of the values of stress at a critical point of the structure obtained during the simulation is shown on Fig. 6.9.

The rainflow procedure proposed by Nieslony [28] was used to determine the quantity of stress cycles per stress block. The obtained histogram and the Weibull probability density function for the stress ranges are shown on Fig. 6.10.

The simulation period was 1000s and it was considered to be representative of a 3 hours sea state for the given significant height.

The drilling tower is built from ten sections with different thickness welded to each other and welded to the deck of the platform. Each section in turn is built from four steel plates with same thickness, as shown on Fig. 4.2. Despite of the recommendation for doing a non-destructive examination after

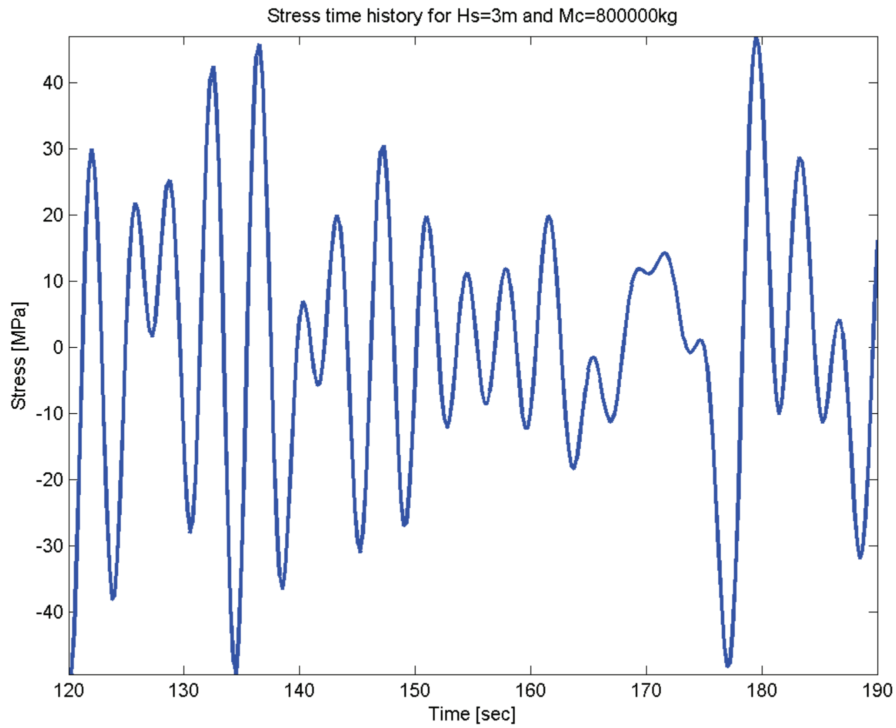

Figure 6.8: Stress time history at critical point

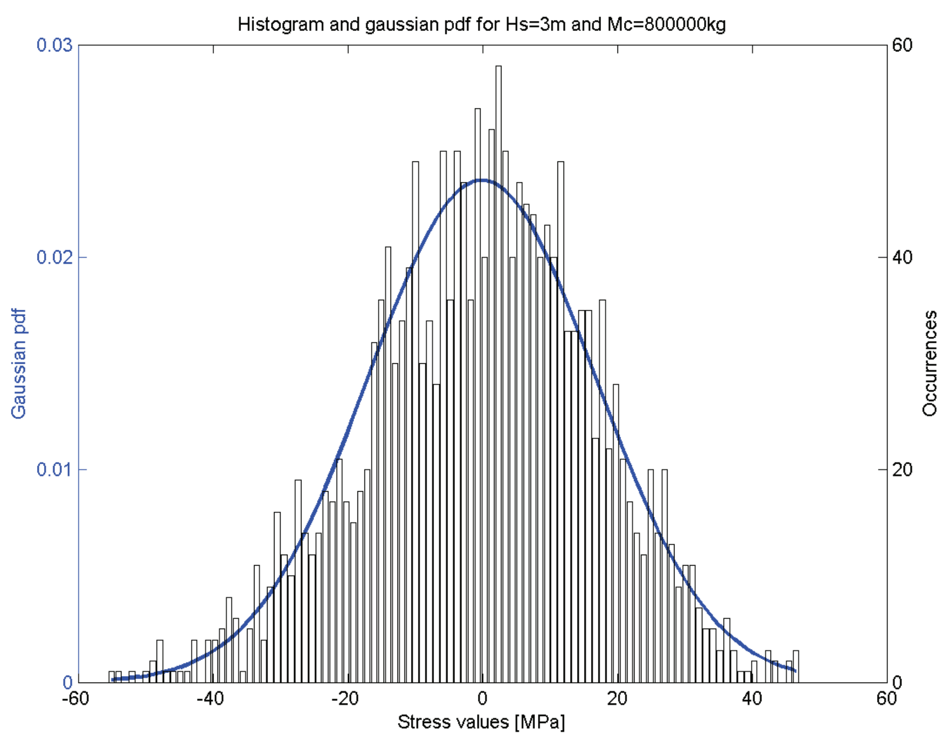

Figure 6.9: Histogram and Gaussian pdf

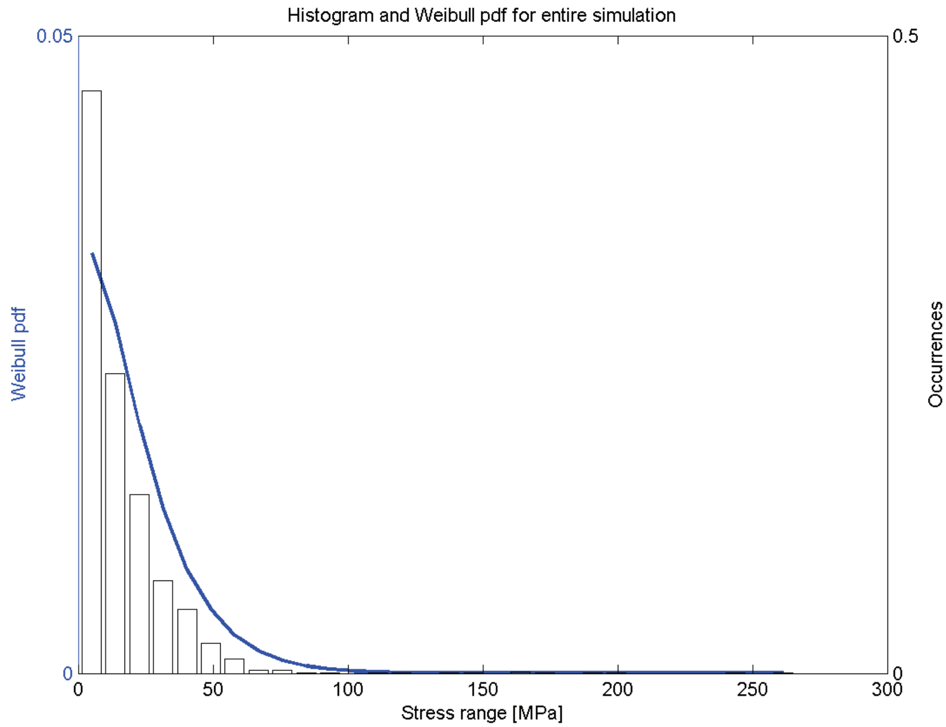

Figure 6.10: Histogram and Weibull pdf for entire simulation

the welding process, [6], there is always some level of misalignment between the plates, and the welds can not be considered to have its nominal thickness all over its length. The thickness of the steel plates is not constant all over its area as well. The thicknesses of the welds between the sections of the tower will be considered a random variable ranging from 80% to 100% of the thickness of the plates. Further, after the welding process there is always some level of residual stress in the welds.

Due to the uncertainty on the manufacturing process of the steel plates, the thickness of the plates within the length of each finite element will be considered a random variable ranging from 100% to 105% of the nominal thickness of the plates. Such variations on the parameters of the structure must be considered during the evaluation of the fatigue resistance of the equipment, otherwise the obtained value may be to conservative. A correlation length of 0.01 between the thicknesses of the different welds and between the thicknesses of the plates within each finite element has been considered.

During the Monte Carlo simulation for the evaluation of the mean value and of the variance of the fatigue resistance it is necessary to simulate all the sea and loading conditions for each trial of the random parameters. Since the quantity of different sea and loading conditions is significant, it is necessary to reduce the computational effort as much as possible. The Tab. 6.4 shows a few statistics for the results obtained after the Monte Carlo simulation

Table 6.4: Influence of the uncertainty

Fatigue Damage					First Natural Frequency [Hz]				
Min.	Max	μ	σ	σ/μ	Min.	Max	μ	σ	σ/μ
0.57	1.04	0.71	0.15	0.21	2.99	3.01	3.00	0.004	0.001

Two MATLAB® programs have been developed to obtain theses results. The first programs evaluates the sea surface elevation, the dynamics of the platform and the excitation on the base of the tower. The second one takes the base excitation, evaluates the dynamics of the drilling tower, including the random variation of the parameters of the tower, and calculates the statistics for the fatigue damage.

Table 6.5: Parameters for MATLAB® programs

Qty. of significant wave heights	8
Qty. of harmonic terms for sea surface elevation	256
Simulated sea surface area	100 x 100 m
Time increment for simulation	0.25 s
Simulation time for each wave direction	600 s
α constant for Newmark method	0.25
Δ constant for Newmark method	0.5
Qty. of terms on KL basis for sea surface reduced-order model	12
Elasticity modulus for steel	2.1E11 N/mm^2
Mass density for steel	7.85E3 kg/m^3
Qty. of finite elements	100
Qty. of degrees of freedom per node	4
Qty. of Monte Carlo simulations for each set of parameters	100
Qty. of eigenmodes for reduced-order model for the drilling tower	30

For each significant wave height 5 wave directions have been simulated during 600s. The initial 120s of each simulation were not considered. The considered simulation for each wave direction were combined in one simulation for each significant wave height. Since the sea surface elevation is an stationary and ergodic process, this unique simulation, and the base excitation obtained considering it, have been used for all Monte Carlo simulations, where only the random parameters of the drilling tower have been drawn.

An histogram of quantity of cycles per stress range has been obtained for each Monte Carlo simulation, and the quantity of cycles obtained during simulation was multiplied by a factor proportional to the relation between the expect working time under each significant wave height and the total simulation time. From the values obtained during Monte Carlo simulation the mean and the variance for the fatigue damage and for the first natural frequency of the drilling tower have been calculated.